AD_____

MIPR NUMBER: 93MM3505

TITLE: Growth Dynamics of Breast Cancer Cells: A Study of Growth Regulatory Factors

PRINCIPAL INVESTIGATOR(S): Bruce C. Veit, Ph.D.

CONTRACTING ORGANIZATION: William Beaumont Army Medical Center
El Paso, Texas 79920-5001

REPORT DATE: January 1996

TYPE OF REPORT: Final

PREPARED FOR: U.S. ARMY MEDICAL RESEARCH AND MATERIAL COMMAND
Fort Detrick, Frederick, Maryland 21702-5012

REPORT DOCUMENTATION PAGE

Form Approved
OMB No. 0704-0188

1. AGENCY USE ONLY (Leave blank)	2. REPORT DATE	3. REPORT TYPE AND DATES COVERED
	January 199	Final (21 Oct 92 - 31 Dec 95)

4. TITLE AND SUBTITLE
Growth Dynamics of Breast Cancer Cells: A Study of Growth Regulatory Factors

5. FUNDING NUMBERS
93MM3505

6. AUTHOR(S)
Bruce C. Veit, Ph.D.

7. PERFORMING ORGANIZATION NAME(S) AND ADDRESS(ES)
William Beaumont Army Medical Center
El Paso, Texas 79920-5001

8. PERFORMING ORGANIZATION REPORT NUMBER

9. SPONSORING/MONITORING AGENCY NAME(S) AND ADDRESS(ES)
Commander
U.S. Army Medical Research and Materiel Command
Fort Detrick
Frederick, Maryland 21702-5012

10. SPONSORING/MONITORING AGENCY REPORT NUMBER

11. SUPPLEMENTARY NOTES

12a. DISTRIBUTION/AVAILABILITY STATEMENT
Approved for public release; distribution unlimited

12b. DISTRIBUTION CODE

13. ABSTRACT (Maximum 200 words)

Primary human breast cancer tissues obtained from biopsies or mastectomies were characterized in terms of DNA content by flow cytometric and digital image analyses and expression of growth factor receptors, e.g. estrogen and progesterone receptors. One breast tumor biopsy was accompanied by an axillary lymph node which contained metastatic tumor. The primary (breast) tumor contained two aneuploid stem lines with DNA indices of 1.4 and 1.9 and S-phase fractions of 19.8% and 7.4%, respectively. Metastatic tumor in the axillary lymph node contained only one aneuploid stem line with an S-phase fraction of 9.6% and a DNA index of 1.7 suggesting the possibility of the emergence of a sub-line in the metastatic tumor.

Flow cytometric analysis of mutant p53 expression of BT-474, DU-4475 and SK-BR3 cells indicated that significant differences existed between these three cell lines in terms of time during culture when p53 is expressed and variations in cell-cycle specific expression. These findings have particular relevance to previous reports which showed that the p53 tumor suppressor gene product is involved in the induction of apoptosis as the result of growth factor deprivation possibly by down-regulating bcl-2 expression.

A DNA 3'-OH digoxigenin-nucleotide end extension-FITC-anti-digoxigenin labeling technique was used for detecting the presence of fragmented DNA in intact cell nuclei as a marker for apoptosis in etoposide-treated BT-474 and MCF-7 cells. Cell cycle analysis indicated that the number of apoptotic cells increased markedly after 16-23 hours of culture and that these cells were detected primarily in the S-phase fraction.

14. SUBJECT TERMS	15. NUMBER OF PAGES
breast cancer, flow cytometry, digital image analysis, p53, BT-474 cells, MCF-7 cells, SK-BR3 cells, apoptosis, digoxigenin-nucleotide labeling	37
	16. PRICE CODE

17. SECURITY CLASSIFICATION OF REPORT	18. SECURITY CLASSIFICATION OF THIS PAGE	19. SECURITY CLASSIFICATION OF ABSTRACT	20. LIMITATION OF ABSTRACT
Unclassified	Unclassified	Unclassified	Unlimited

FOREWORD

Opinions, interpretations, conclusions and recommendations are those of the author and are not necessarily endorsed by the US Army.

____ Where copyrighted material is quoted, permission has been obtained to use such material.

____ Where material from documents designated for limited distribution is quoted, permission has been obtained to use the material.

BCY Citations of commercial organizations and trade names in this report do not constitute an official Department of Army endorsement or approval of the products or services of these organizations.

BCY In conducting research using animals, the investigator(s) adhered to the "Guide for the Care and Use of Laboratory Animals," prepared by the Committee on Care and Use of Laboratory Animals of the Institute of Laboratory Resources, National Research Council (NIH Publication No. 86-23, Revised 1985).

BCY For the protection of human subjects, the investigator(s) adhered to policies of applicable Federal Law 45 CFR 46.

____ In conducting research utilizing recombinant DNA technology, the investigator(s) adhered to current guidelines promulgated by the National Institutes of Health.

____ In the conduct of research utilizing recombinant DNA, the investigator(s) adhered to the NIH Guidelines for Research Involving Recombinant DNA Molecules.

BCY In the conduct of research involving hazardous organisms, the investigator(s) adhered to the CDC-NIH Guide for Biosafety in Microbiological and Biomedical Laboratories.

Bruce C. Yeh 4/10/96

PI - Signature Date

TABLE OF CONTENTS

INTRODUCTION

Breast cancer is a major cause of death among women in the United States. Annually, about 1 in 9 women are diagnosed with breast cancer and approximately 50,000 women die of breast cancer each year. Although incidence rates slightly increase each year, early detection and improved treatment have kept mortality rates fairly stable over the past 50 years. The 5-year survival rate for localized breast cancer has risen from 78% in the 1940's to over 90% today; for women with in situ (non-invasive) breast cancer, the survival rate approaches 100%. However, women with breast cancer that has spread regionally have a survival rate of about 70% and those with disseminated (distally spread) cancer have a very poor survival rate of only about 20%. Since tumors with high proliferation rates correlate with poor prognosis, new approaches with S-phase-specific chemotherapeutic agents are being pursued in an attempt to improve survival in women with more rapidly growing and metastasizing tumors. One such approach is through the use of agents which induce apoptosis.

Apoptosis is a naturally-occurring physiological, "programmed" cell death that is mechanistically distinct from necrosis. Whereas necrosis is associated with accidental or pathological cellular injury resulting from a general failure of cellular homeostatic regulation following injury, apoptotic mechanisms are involved in several homeostatic systems which regulate normal cell growth, e.g. maturation of the immune system, embryonic development, hormone deprivation of endocrine or other hormone-dependent or sensitive cells, cells responding to mild thermal or metabolic stress, and normal tissue turnover (1 - 8).

Mechanistically, apoptosis involves the active participation of inducible cells which carry out their pre-programmed self-destruction when appropriately signaled to do so. Upon stimulation by apoptosis-triggering agents, susceptible cells, with specific response pathways, will activate a pre-programmed cascade of molecular and biochemical events, which are accompanied by characteristic morphologic changes that terminate in cell disintegration (3,9 - 11).

Numerous morphological and biochemical differences distinguish apoptosis from necrosis, two alternative pathways which lead to cell death (12,13). The apoptotic process involves a sequence of cell shrinkage, increased cytoplasmic density, chromatin compaction, and segregation into sharply circumcised masses that abut on the nuclear membrane and can form blister-like protrusions. The latter then separate to produce membrane-bound apoptotic bodies. Initially, mitochondria and the Golgi apparatus show no signs of swelling and the nuclear membrane remains intact for an extended period of time. In contrast, necrotic cells show chromatin clumping into ill-defined masses, gross swelling of organelles and at a later stage membrane breakdown and cell disintegration. These morphological changes can be detected using the electron microscope. Morphological examinations, however, all have the same disadvantage in that they are qualitative but not quantitative. Most published reports are consistent with these distinctions between apoptosis and necrosis but other variant forms of cell death have also been described (1,3).

A key morphological feature of apoptotic cell death is the condensation of chromatin and its margination at the nuclear periphery (10). The biochemical hallmark of apoptosis is the appearance of a fragmentation pattern in chromatin indicative of the DNA cleavage at linker regions between nucleosomes. The multistage process of DNA fragmentation is typically associated with morphologic apoptosis. In a number of well-researched model systems, large fragments of 300kb and 50kb are first produced by endonucleolytic degradation of higher-order chromatin structural organization. These fragments are visible on pulsed-field electrophoresis gels (14, 15). Then, in most experimental models, the activation of Ca++ and Mg++ dependent endonuclease activity further cuts about 30% of the chromatin by cleavage at linker DNA sites between nucleosomes

(16). The ultimate DNA fragments are multimers of 180 - 200bp nucleosomal units, resulting in the appearance of "DNA laddering" in standard agarose gels of DNA extracted from many kinds of apoptotic cells (11,17 - 19). Digoxygenin-nucleotide labeling of 3'-OH ends of fragmented DNA is an alternative method of detecting apoptosis (19,20 - 23). Since the single-cell sensitivity of digoxigenin-nucleotide labeling is far higher than that of standard DNA agarose gel electrophoretic analysis, it is a more useful method for detecting small numbers of apoptotic cells, particularly when in situ determinations are required.

There is a wide variety of agents that have been reported to induce apoptosis in a number of different types of cells and tissues. Tumor necrosis factor (TNF-α) has been shown to promote an increase in intranuclear free CA++ which, in turn, can stimulate Ca++-dependent endonuclease activity resulting in DNA fragmentation and apoptosis (24). Estrogen deprivation resulting in biochemical and morphological changes characteristic of apoptosis in estrogen-responsive MCF-7 cells has been shown to cause tumor regression in nude mice (25). Anti-cancer drugs such as the topoisomerase inhibitors, camptothecin (topoisomerase I inhibitor) and VP-26, etoposide and the more potent VM-26, teniposide (topoisomerase II inhibitors) as well as physical agents such as hyperthermia and γ-irradiation have all been shown to trigger apoptosis in HL-60 myelogenous leukemia cells and other cells (26). The various apoptosis-inducing agents appear to be cell-cycle phase-specific in their mode of action. Hyperthermia preferentially induces apoptosis in G_1 whereas γ-irradiation triggers apoptosis primarily in G_2 + M cells. Topoisomerase inhibitors appear preferentially inhibit cells traversing S-phase and have little or no effect on cells in G_1 or G_2 phases (27,28).

It is becoming clear that the effectiveness of anti-tumor drugs is dependent on the intrinsic ability of tumor cells to undergo apoptosis (29,30). This ability appears to correlate with the proliferative status of the tumor cells specifically in terms of oncogene expression such as *bcl-2*, *c-myc*, p53 or *c-ras* (31). The protein product of the wild-type p53 suppressor gene is believed to be involved in the induction of apoptosis in cells with significant amounts of DNA damage caused by x-irradiation or chemotherapy (32). These molecules have also been reported to play a role in the induction of apoptosis in growth factor-deprived cells (33) possibly by down-regulating *bcl-2* and upregulating the expression of the *bax* protein in breast cancer cells (34,35).

In spite of aggressive chemotherapy, breast tumor cell populations which have high proliferation rates (contain large S-phase fractions) are frequently associated with metastasis and poor prognosis. As the size of the S-phase fraction for a given tumor cell population increases, there is a predictable increase in the frequency with which mutational changes will occur. Such changes may cause the tumor cell population to acquire new growth requirements, altered responsivity to growth-promoting or apoptosis-inducing stimuli, or altered susceptibility to anti-cancer drugs.

Our studies are primarily aimed at developing methods of increasing tumor cell killing through the use of agents which accelerate S-phase cytotoxicity via apoptosis induction. The primary breast tumor characterization studies to be described first were carried out for the purpose of establishing an initial tumor cell profile which would include DNA content (cell-cycle analysis) and growth factor/receptor expression. These profiles were then to be used for comparison with subsequent profiles carried out on the primary tumor cell population which had been grown in nude mice and/or on metastatic tumor cells from the primary breast tumor patients. These studies were partially completed in that we were able to obtain profiles on several primary tumor cell populations but the xenograft studies in nude mice and the metastatic tumor profiles were not done. The second series

of experiments to be described were focused on the development of an in vitro model to study the induction of apoptosis in breast cancer cells using and S-phase-specific inhibitor of DNA synthesis (etoposide) which has also been shown to induce apoptosis in myelogenous leukemia cells as mentioned above.

BODY

1. Primary Human Breast Cancer Biopsies

Primary breast tissue (normal or malignant) was obtained from surgical biopsy and/or mastectomy. In some cases where mastectomy was performed, portions of the tumor and normal breast tissues were obtained and co-processed. When possible, freshly collected tissues were divided into portions for DNA analysis by flow cytometry and digital imaging, for implantation in nude (athymic) mice, and for fixation and paraffin embedding and/or frozen storage for archiving and other studies.

Table 1 lists 19 malignant tumors obtained in which there was sufficient tissue for analysis. In one case, TI0007, a portion of the patient's axillary lymph node was also obtained for study (TI0008).

Presence or absence of detectable estrogen or progesterone receptors was determined for each tissue. 5 um sections of formalin-fixed, paraffin-embedded tissues were de-paraffinized, re-hydrated, treated with 0.05% trypsin for 8 minutes at 37°C followed by treatment with Antigen Retrieval Citra solution (Biogenex) in a microwave at high power for 10 minutes. Tissue sections were then incubated for 2 hours at room temperature with monoclonal mouse anti-estrogen receptor antibody (clone ERID-5, Arnac, Inc.), monoclonal mouse isotype Ig or monoclonal mouse anti-vimentin (Biogenex), then for 20 minutes at room temperature with biotinylated goat anti-mouse Ig followed by incubation with peroxidase ~ anti-peroxidase complex for 20 minutes at room temperature and finally with AEC substrate for 5 - 40 minutes at room temperature until optimal color intensity was achieved. Tissue sections were then stained with Mayer's hematoxylin, cover-slip mounted with Crystal Mount and evaluated. ER nuclear immunostaining was either negative (-), light (1 - 2+), intermediate (2 - 3+), or intense (4+). Levels of intensity were quantitated by digital image analysis using a Roche Image Analysis Workstation. The percentage of immuno-positive nuclei in a minimum of 200 tumor cells was estimated at 40x magnification in an area of maximal staining. Cytoplasmic staining was considered to be non-specific. Vimentin-stained control slides were used to validate tissue preparation and antigen retrieval. Figure 1 shows a tissue section of a patient with intraductal carcinoma. As shown, intraductal tumor nuclei are 4+ reactive for estrogen receptor. The procedure for detecting progesterone receptors (PR) was essentially the same as that described for ER with the exceptions that monoclonal mouse anti-progesterone receptor (clone NCL-PGR, Biogenex) was used as the primary antibody, streptavidin~alkaline phosphatase was used as the linking reagent, and New Fuchsin + levamisole was used as substrate. Evaluation was the same as that for ER.

There was sufficient tissue in 9 of the 19 samples for implantation via trocar into the mammary fat pads of nude (athymic) mice as described by Price et al (36). Unfortunately, 0 of 9 implants developed tumors in the xenografted mice. In some cases, tumors did not grow because the implanted specimens were subsequently found to contain either fatty tissue or normal epithelial tissue. In other cases, it is likely that the xenograft failures (later determined to involve ER+ tissues) were due to the lack of a suitable estrogen-enriched environment (recipient mice were not routinely treated with estrogen). A recent report (37) has indicated that estrogen supplementation enhances

tumorigenicity somewhat but a much greater level of tumorigenicity was obtained when breast cancer cells were co-inoculated with estrogen and basement membrane matrix (Matrigel). In future attempts to grow xenografted primary breast cancer tissue, we will incorporate these findings into our protocol. We were successful in growing two established breast cancer cell lines, BT-474 and DU-4475, as tumor xenografts in nude mice. It is likely that our success rate in growing xenografted breast cancer cells from established cells lines will also increase when we combine the cell implants with estrogen and basement membrane matrix.

The use of xenografted primary breast cancer tissue implants in nude mice represented a major portion of our study of the influence of growth factors on the growth and evolution of breast cancer cells. Because of failures in our early attempts to grow primary human breast cancer xenografts in nude mice and because of the lack of funding (which ended October 1994) to continue this aspect of our studies, we suspended further work in this area and focused our attention primarily on in vitro studies of breast cancer cell lines and the detection of drug-induced apoptosis which will be described later.

2. DNA Analysis of Primary Human Breast Cancer Tissues

A. Flow Cytometry

The following studies were conducted to partially address the issue of establishing parent (primary) breast tumor cell profiles consisting of DNA content and cell cycle characteristics and growth factor/receptor expression as determined by flow cytometric and digital image analysis. This information was to be used in further studies of metastatic tumors from these patients and tumor cell heterogeneity studies in nude mouse xenografts to determine the extent to which new clones of breast cancer cells with different DNA and/or growth factor characteristics evolve during in vivo growth. Results described below are from flow cytometric and image analysis studies of DNA content of primary breast tumor samples.

To study DNA content and cell cycle characteristics of primary breast tumor samples from patients, the method of Dressler et al (38) which was optimized for analysis of breast cancer samples was used. For mechanical disaggregation, fresh or frozen (snap frozen in liquid nitrogen and stored at -70°C) tissues were placed in cold 1.12% citrate buffer and cut in half with a #20 scalpel blade. The freshly cut surface was scraped with the edge of a glass microscope slide and cells were released into the medium. In some preparations, a Medicon Tissue Disaggregator (Consul T.S. Di Roggero Gianmarco & Co, Bruino, Italy) with a #10 blade was used to prepare single cell suspensions from fresh or frozen tissues. Cell suspensions were filtered through 53-micron nylon mesh, washed and 1 to 5 x 10^5 cells fixed with 100 ul 95% ethanol. Fixed cells were then treated with propidium iodide in Krishan buffer for 60 minutes at 4°C in the dark, filtered through 37-micron nylon mesh using a syringe and a 27 gauge needle and analyzed by flow cytometer. When initial propidium iodide screening indicated that the tumor was aneuploid, then the gated aneuploid population was analyzed. If the initial screening indicated that the tumor was diploid, then the tumor cells were stained for cytokeratin by incubating propidium iodide-stained cells with fluorescein (FITC)-labeled anti-cytokeratin for 15 minutes at room temperature in the dark. Cytospin preparations of each cell suspension were stained with Papanicolaou stain for cytologic evaluation of tumor cell content.

DNA analysis was performed essentially as described by Dressler (39). Normal human peripheral blood lymphocytes (obtained by Ficoll-Paque separation of heparinized blood) were added to sample tubes as an internal standard prior to staining with propidium iodide. An internal standard was used to normalize the histogram and to identify the position of human diploid G_0/G_1

nuclei. In some cases, the presence of normal breast epithelial cells also served as a G_0/G_1 diploid reference. The DNA index (DI) was determined by dividing the modal channel number of the aneuploid G_0/G_1 DNA peak by the modal channel number of the diploid G_0/G_1 DNA peak. Validation of reliable tumor analysis required that cytologic evaluation revealed the presence of < 15% tumor cells. A diploid DNA histogram showed a single G_0/G_1 peak with a CV < 5% and a corresponding G_2M peak whose diploid position was confirmed by the DNA histogram of the internal standard. An aneuploid histogram showed one or more discrete G_0/G_1 peaks with CVs < 5% which did not correspond to the G_0/G_1 peak of the diploid internal standard or that of normal breast epithelial cells The aneuploid G_0/G_1 peak(s) contained at least 5 - 10% of the total events collected and had corresponding G_2M peak(s) that were identifiable. Modfit Version 5.11 (Verity Software House, Inc., Topsham, Maine) DNA modeling software was used for single-parameter DNA histogram cell cycle analysis.

Table 2 shows the results of cell cycle analyses of the primary human breast cancer tissues described in Table 1. Several tissues analyzed (TI0001, 4, 9, 25, 26, 33, and 36) contained only normal epithelial cells with no detectable aneuploid (tumor) cells. Of particular note is tissue TI0007 which apparently contained two aneuploid stem lines with DIs of 1.4 and 1.9. Of interest is the finding that the stem line with a DI of 1.4 had an S-phase fraction of 20% whereas the other stem line had an S-phase fraction of 7%. Tissue TI0008 was a portion of an axillary lymph node from the patient with TI0007 breast tumor biopsy. In this tissue, only one stem line was identified which had an S-phase fraction (10%) that was similar to the second aneuploid stem line of TI0007 but the DI was 1.7 rather than 1.9 suggesting the possibility of the emergence of a sub-line in the metastatic tumor.

3. Image Analysis

DNA content and cell cycle characteristics of primary breast tumor samples from patients were also studied by digital image analysis. Tissue samples were processed by mechanical disruption to obtain single-cell suspensions as described above for flow cytometric analysis. Suspended cells were then deposited onto microscope slides with a cytospin centrifuge. In addition, touch imprints were prepared from freshly cut fresh or frozen tumor tissues. Imprints or cytospin preparations were immediately fix in 10% neutral buffered formalin for 30 minutes, washed in running deionized water for 5 minutes, air dried and stored at room temperature until they were stained. Cellular DNA was hydrolyzed with 5N HCl for 60 minutes at room temperature then cells were incubated with Feulgen reagent (Roche Image Analysis Systems) for 60 minutes at room temperature. Cytoplasmic clarification was performed by placing the samples in a 1% HCl - ethanol solution for 5 minutes. The samples were then dehydrated in ethanol, cleared with xylene, cover-slip mounted with Permount, and evaluated by digital image analysis. DNA quantitation by digital image analysis relies on specific and stoichiometric binding of the Feulgen reagent to DNA. HCl hydrolyzes ribose-purine bonds in DNA to yield sugar aldehyde residues. Feulgen reagent then binds to the sugar aldehyde groups via a Schiff reaction to give a blue color. The quantity of blue color associated with DNA is stoichiometrically proportional to the amount of DNA present in a cell. DNA quantitation is based on the assignment of an optical density to each subunit (pixel) of the nuclear image and obtaining the sum of all optical densities of the pixels for each nucleus. The sum of these optical densities, or integrated optical density (IOD), corresponds to the total amount of DNA in each cell. At least 200 tumor cells for each sample were analyzed. DNA indices (DIs) were calculated by dividing the mean IOD of the aneuploid G_0/G_1 cell peak by the mean IOD of the

normal diploid cell control. In cases where the tumor sample contained sufficient normal breast epithelial cells, the mean IOD of these cells, serving as an internal standard, was used for calculating DIs. In those cases where there were not sufficient normal cells present in the tumor sample, the mean IOD of an external standard (determined from normal breast tissue samples) was used for calculating DIs.

Table 3 shows the results of testing three different normal cell types that are used for DNA quantitation by image analysis. Mean IODs for breast epithelial cell DNA, peripheral blood mononuclear cell DNA, and rat hepatocyte DNA were 163.5, 158.3, and 134.1, respectively. The mean IODs of all three populations were statistically significantly different from each other. Although it was possible to "normalize" the IOD values of rat DNA or peripheral blood mononuclear cell DNA with that of normal breast epithelial cells thereby allowing us the use of readily obtainable external reference cell DNA, we decided to use internal or external normal breast epithelial cell DNA as our reference for estimating the DIs of the tumor tissue. Since some of the samples to be analyzed for DNA content were frozen, it was of interest to determine if significant differences occurred between fresh and frozen tissues prepared by touch imprinting or mechanical disaggregation. Shown in Table 3, are the mean IOD values for five normal breast tissue samples that were each prepared as either fresh or frozen touch imprints or fresh or frozen mechanically desegregated cell suspensions. Regardless of the variations in cell preparation, there was no statistically significant difference observed between the mean IODs of all of these preparations.

Table 4 shows the results of digital image DNA analysis of the evaluable primary breast cancer tissues listed in Table 1. Tissue samples TI0004, 24, and 26 with DNA indices of 1.0 contained no detectable aneuploid cells as was observed when these samples were also analyzed by flow cytometry (see Table 2). Mean IOD values are listed for the external reference normal breast epithelial cell DNA (164) and for each internal reference when the tissue samples contained sufficient numbers of normal breast epithelial cells for evaluation. As can be seen, there was good concordance between DNA indices that were calculated with the external reference IOD and DNA indices calculated with the internal reference IOD. Furthermore, there was consistent agreement between the DNA indices observed by flow cytometry and those obtained by image analysis (see Table 2 for flow cytometric results). The two aneuploid stem lines observed in TI0007 by flow cytometry (see Table 2) were also observed by image analysis. Tissue TI0008, a portion of an axillary lymph node from the patient from whom the TI0007 tumor biopsy was obtained, again exhibited a single, putative variant aneuploid sub-line of the two aneuploid stem lines observed in TI0007. Further studies of frozen and paraffin-embedded tissues from this patient are in progress to provide a better understanding of these findings.

3. In Vitro Studies of Human Breast Cancer Cell Lines

It is generally recognized that there are significant differences between cultured breast cancer cell lines and primary breast tumor cells in terms of growth properties, clonality, micro-environmental influences (present in vivo and absent in vitro), morphology, and other factors. Although in vivo studies provide more relevant information relating to natural growth processes, they are somewhat restrictive in terms of availability of study tissues, constancy of growth characteristics, and several other properties. For these reasons, certain in vitro studies of breast cancer cell lines were undertaken in order to establish a tumor cell model for studies of apoptosis which would then be applied to future in vivo studies. The following results were obtained from studies focused on the evaluation of several established breast cancer cell lines for use in developing such a model. It should be pointed out that the DNA analyses to be described were

carried out on non-synchronized cell cultures. Therefore, cell cycle compartmentalization data do not represent cohorts of cells as they pass through different cell cycle phases.

Several established human breast cancer cell lines were obtained from the American Type Culture Collection (ATCC) and were maintained in continuous in vitro culture for use in studies of the induction of apoptosis.

BT-474 is a human breast ductal carcinoma cell line that was originally established by Lasfargues and Coutinho (40) from a solid, invasive ductal carcinoma of the breast. The cell line was maintained in RPMI 1640 containing 10 mg/L bovine insulin, 300 mg/l L-glutamine, and 10% fetal bovine serum. These cells grow as compact, multi-layered, adherent patches of epithelial cells which do not become confluent. We were able to grow tumor xenografts with this cell line in nude mice.

MCF-7 is a human breast adenocarcinoma cell line that was originally established from a pleural effusion by Soule et al (41). This cell line is maintained in RPMI 1640 containing 10 mg/L L-alanine, 1mM sodium pyruvate, and 10 mg/L bovine insulin, and 10% fetal bovine serum. These cells utilize estradiol through cytoplasmic estrogen receptors.

MDA-MB-231 is a human breast adenocarcinoma that was originally established from a pleural effusion by Cailleau et al (42). This cell line was maintained in Leibovitz's L-15 medium containing 10 % fetal bovine serum.

SK-BR-3 is a human breast adenocarcinoma that was originally established from a pleural effusion by Trempe and Old in 1970. This cell line was maintained in RPMI 1640 containing 10 mg/L L-alanine and 10% fetal bovine serum.

DU-4475 is a human breast carcinoma originally established by Langlois et al (43) from a metastatic cutaneous nodule from a patient with advanced breast cancer. This cell line is maintained in RPMI 1640 containing 20% fetal bovine serum. These epithelial-like cells grow in suspension as clusters or aggregates with serpentine-like outgrowths. We were able to grow tumor xenografts with this cell line in nude mice.

Table 5 shows the results of flow cytometric and digital image analysis of the DNA content of these five cell lines when processed during logarithmic growth. For image analysis, calculation of DNA indices for these tumor cell lines was with a mean IOD value of 164 for normal breast epithelial cell DNA. There was good correlation between percentages of cells in the three cell cycle compartments when analyzed by image analysis and flow cytometry and DNA indices correlated well between the two methods of detection. Table 5 also shows the results of DNA analyses of one of the xenografted tumors that was derived from an injection of DU-4475 cells and excised from a nude mouse 25 days after injection of the cells. Again, results of flow cytometric and image analyses correlated well with regard to DNA indices. In vitro grown DU-4475 cells had a DNA index of 2.0 (image) and 2.1 (flow). The xenografted tumor had DNA indices of 2.0 and 2.1, respectively. Interestingly, the S-phase fraction of the tumor xenograft was 22% (25% by flow analysis) whereas in vitro cultured cells had an S-phase fraction of 17% (16% by flow analysis). The increase in S-phase cells is most likely due to enhanced growth in a more favorable environment (in vivo vs. in vitro).

One of the cell lines, BT-474, was selected for further studies (including those of apoptosis to be described later). Since it was reported that this cell line required the presence of insulin as a growth requiring factor, cell cultures were established in the presence and absence of 10 mg/L bovine insulin and viable cell numbers as well as DNA analyses were performed at varying times during culture. Since these cells grow as an adherent, epithelial-like population and detachment or non-adherence is associated with cell death (and presumably apoptosis to some extent), it was of interest to quantitate numbers of adherent and non-adherent cells at various times during culture.

Results of this experiment are shown in Table 6. At the initiation of culture, 1 x 10^6 cells per flask were seeded. Six hours later, relatively few cells were non-adherent when grown either in the presence or absence of insulin presumably because these cells were in the process of dying at the time of culture initiation and failed to attach. After 1 day of culture, there was a significantly higher number of cells growing in the presence of insulin when compared to that of insulin-deprived cultures. As time progressed, the number of non-adherent cells in insulin-deprived cultures rose rapidly compared to that of insulin-supplemented cultures with a corresponding rapid increase in the adherent cell population in the latter cultures and a much slower and gradual rise in insulin-deprived cultures. Although BT-474 cells were able to grow slowly in insulin-deprived cultures, their growth rate was greatly inhibited. Results of DNA analysis of the cells growing in the presence of insulin are also shown. Curiously, the DNA indices of this cell line appeared to increase with time in culture from 2.1 on day 0 to 2.6 on day 11. There was also a significant change in the S-phase fraction during culture with the percentage of 24 at the initiation of culture decreasing to 12 by day 11. This two-fold drop in the S-phase fraction is most likely due to a decline in cell growth overall in these cultures since the number of viable non-adherent cells on day 11 was 120 x 10^5 whereas, on day 9 it was 143.3 x 10^5.

4. Expression of Mutant p53 Gene Product in Cell Cycle Compartments of BT-474, DU-4475, and SK-BR3

The product of the p53 tumor suppressor gene has been reported to be involved in the induction of apoptosis. Lowe et al (44) has reported that the wild-type p53 gene product plays an important role in the induction of apoptosis in cells which have sustained a significant amount of DNA damage from x-irradiation or chemotherapy. The p53 gene product has also been shown to play a role in the induction of apoptosis by growth factor deprivation (33) possibly by down-regulating bcl-2 expression (34). It has also been reported that BT-474 cells have undergone a missense mutation in the p53 gene resulting in the loss of heterozygosity (45). It is unclear what effect the loss of wild-type p53 in BT-474 cells has on the involvement of mutant p53 in the induction of apoptosis. Table 7 shows the results of flow cytometric analysis of mutant p53 expression in cell cycle compartments of BT-474, DU-4475 and SK-BR3 cells at various times during a 7-day growth period. Regardless of the time in culture and cell cycle compartment, almost all BT-474 cells expressed mutant p53 gene product indicating that the expression of these molecules is not modulated by growth of BT-474 cells. By contrast, DU-4475 and SK-BR3 cells did exhibit variations in the expression of mutant p53 gene product during their growth. On day 0 of culture, 16% of DU-4475 cells expressed this protein. The percentage rose to 86% on day 1 and declined to 19% by day 7. The percentage of cells in each compartment of the cell cycle exhibited similar increases and decreases. There appeared to be no preferential expression in specific phases of the cell cycle. SK-BR3, on the other hand, exhibited a 41% expression of mutant p53 on day 0 which rose to 98% by day 1 and remained elevated through day 7. Interestingly, there appeared to be an up-regulation of the expression of this protein in G_0/G_1 and S phases of the cell cycle by day 1, but its expression in G_2/M cells was 96% on day 0 and remained the same throughout the 7-day culture period. It should be mentioned that the DNA analyses in these and other studies described in this report were of non-synchronized cells. The percentages of cells for each cell cycle compartment in Table 7, as well as those described in other studies in this report, are approximate and require repeated measurement under the same conditions in order to establish reproducibility and statistical reliability.

5. Induction of Apoptosis With Heat, Camptothecin, TNF-α, and Etoposide

A major goal of our research is to establish a model system for studying the involvement of apoptosis in breast cancer cell death. An essential aspect of this model is the development of methods for detecting apoptotic cells. The most distinguishing feature of apoptosis is the internucleosomal cleavage of DNA into fragments of 180 - 200bp (apoptotic bodies) via the activation of an endonuclease or endonucleases. Morphologically identifiable nuclei with fragmented DNA (those containing apoptotic bodies) contain newly exposed 3'-OH DNA ends. By contrast, normal or proliferative nuclei with no apoptotic bodies have few if any exposed 3'-OH DNA ends. Newly exposed 3'-OH DNA ends generated by DNA fragmentation during apoptosis represents a labeling target to which residues of digoxigenin-nucleotide can be catalytically added by terminal deoxynucleotidyl transferase (TdT).

In our studies, apoptotic cells were identified by first carrying out 3'-OH end-extension of DNA fragments with digoxigenin-labeled nucleotides in situ (in intact cells). In this procedure, residues of digoxigenin-nucleotides are catalytically added to DNA fragments by terminal deoxynucleotidyl transferase (TdT), an enzyme which catalyzes template-independent addition of deoxyribonucleotide triphosphate to the 3'-OH ends of double- or single-stranded DNA (20). Following digoxigenin-nucleotide-extension, cells were incubated with anti-digoxigenin antibodies conjugated with FITC. Cell preparations were also labelled with propidium iodide to determine total DNA as a function of cell cycle position. Cells prepared in the above-described manner were then analyzed by two-parameter flow cytometry to identify fluorescent-positive "apoptotic cells" (those cells with DNA strand breaks) and cell cycle compartment within which these cells occur at the various incubation times analyzed. It is not yet known whether this technique is able to specifically detect early-stage apoptosis when chromatin condensation is present but strand breakage is minimal. It is also important to point out that our measurements of apoptosis by this technique require independent confirmation by other techniques to establish the reliability of 3'-OH DNA end labeling in the detection of apoptotic cells.

A wide variety of agents including x-irradiation, glucocorticoid hormones, phorbol esters (TPA), hyperthermia, TNF-α, and several chemotherapeutic drugs such as etoposide (VP-16), teniposide (VM-26), camptothecin, and 5-azacytidine have been reported to induce apoptosis in a variety of cells and tissues. Table 8 shows the results of subjecting BT-474 cells, DU-4475 cells, or MCF-7 cells to various apoptosis-inducing agents: TNF-α, camptothecin, etoposide or hyperthermia. Incubation of BT-474 cells at 43°C for 15 to 60 minutes resulted in 53 to 65% apoptotic cells following an 18 hour incubation. Incubation of DU-4475 cells for 6 hours in the presence of 100 ng/ml TNF-α resulted in approximately 30% apoptotic cells. Camptothecin induced apoptotic cells in both BT-474 cells and DU-4475 cells when present in cultures at 0.1 to 0.2 uM concentrations for 6 or 18 hours. The DNA topoisomerase II inhibitor, etoposide (VP-16), was present in cultures of BT-474 cells and MCF-7 cells for 6, 18, 24, 30, and 45 hours. Unlike the other agents described above that induced apoptotic cells within 6 hours following their addition to culture, significant percentages of apoptotic cells were not observed until 18 hours following the addition of etoposide to cultures. Both BT-474 cells and MCF-7 cells were susceptible to the induction of apoptosis by etoposide. Figure 2 shows Papanicolaou-stained BT-474 cells that were incubated with DMSO for 18 hours. Note the presence of mitotic figures and the typical multi-nucleoli-containing nuclei of these cells. Figure 3 shows Papanicolaou-stained BT-474 cells that were incubated with 85 uM etoposide for 18 hours. Note the presence of nuclei containing several dense "spherules" of chromatin, presumably condensed DNA fragments, that are associated with

the apoptotic process. Figure 4 shows a Papanicolaou-stained preparation of BT-474 cells that were incubated for 45 hours with 85 uM etoposide. As can be seen, there is much more extensive chromatin condensation with many nuclei containing what are presumed to be multiple "spherules" of condensed DNA fragments.

6. Growth of BT-474 Cells and MCF-7 Cells in Etoposide and Studies of Apoptotic Cells

Further studies were carried out to determine the effects of etoposide on cell growth. Figure 5 shows the numbers of viable BT-474 cells observed during a 3-day culture period in the presence of 85 uM etoposide or DMSO as a control (DMSO was used as the solubilizing agent for etoposide). Culture flasks (25 cm^2 growth area) were seeded with 5 x 10^5 BT-474 cells and incubated for 5 days with refeeding on day 3 to establish a stable growth population. On day 5, 85 uM etoposide or DMSO were added to the flasks and incubation continued for an additional 70 hours. As shown in Figure 5, cells incubated with etoposide exhibited a gradual, progressive decrease in viable cell number which began 23 hours after addition of the drug. Cells incubated with DMSO progressively increased in numbers of viable cells during this same period of time.

Since adherence is a key feature of BT-474 growth, it was of interest to determine whether etoposide accelerated cell detachment and, if so, whether detach cells remained viable. Figure 6 shows the results of incubating BT-474 cells in the presence of DMSO or 85 uM etoposide and determining the numbers of viable (trypan-blue dye-excluding) adherent and nonadherent cells during an 88-hour culture period. Since BT-474 cells normally grow as an adherent population, almost all viable cells in the DMSO-treated cultures remained adherent throughout the entire incubation period. By contrast, the etoposide-treated adherent cell populations began decreasing in viable cell numbers by 16 to 23 hours after addition of etoposide to the cultures. Interestingly, there was a corresponding increase in numbers of viable non-adherent cells in etoposide-treated cultures which peaked at about 40 to 45 hours of incubation and then decreased thereafter. Apparently, the presence of etoposide resulted in the detachment of viable cells between 16 to 23 hours of incubation. Figure 7 shows percentages of viable cells in adherent and non-adherent sub-populations of BT-474 cells incubated with DMSO or etoposide. As mentioned above, adherent cells incubated with DMSO remained almost 100% viable throughout the culture period. Adherent cells incubated with etoposide decreased in percentage of viable cells with a corresponding increase in percentage of non-adherent viable cells. It is important to note that the numbers of viable cells decreased after 40 - 45 hours of incubation (see Figure 6). Also shown in Figure 7 are percentages of apoptotic cells in DMSO- and etoposide-treated cultures. After 16 to 23 hours of culture, the percentages of apoptotic cells increased significantly in etoposide-treated cultures reaching an approximate peak of 75% by 70 hours of incubation.

Figure 8 shows the results of two-parameter flow cytometric analyses of DNA content and 3'-OH-end-labeled fluorescent-positive (apoptotic) BT-474 cells incubated with DMSO or 85 uM etoposide. As can be seen, the highest number of apoptotic cells was observed at approximately 20 to 30 hours of culture in the presence of etoposide. Thereafter, the numbers of these cells decreased significantly. Similarly, a dramatic increase in numbers of apoptotic cells was observed in the three cell cycle compartments (G_0/G_1, S and G_2/M) during this same time period with the highest number occurring in the S-phase compartment. Whereas the number of apoptotic S-phase cells appeared to decrease after 23 to 30 hours of incubation, the numbers of G_0/G_1 and G_2/M apoptotic cells remained at constant levels throughout the remainder of the culture period.

Since preliminary studies indicated that MCF-7 cells were also susceptible to the effects etoposide in the induction of apoptotic cells, it was of interest to determine whether the

development of apoptotic MCF-7 cells was similar to that of BT-474 cells. Figure 9 shows the results of quantitating the numbers of viable adherent and non-adherent MCF-7 cells incubated with DMSO or 85 uM etoposide for 70 hours. In general, the kinetics of the growth curves for adherent MCF-7 cells cultured in the presence of DMSO or etoposide are quite similar to those of BT-474 cells (compare with Figure 6). There was, however, a significant difference in the growth of nonadherent MCF-7 cells incubated with etoposide when compared to growth of non-adherent BT-474 cells. Whereas non-adherent BT-474 cells incubated with etoposide exhibited a marked increase in numbers from 16 to 40 hours of culture and decreased thereafter (see Figure 6), non-adherent MCF-7 cells only exhibited a minimal and gradual increase in number throughout the entire culture period. Figure 10 shows percentages of viable cells in adherent and non-adherent sub-populations of MCF-7 cells incubated with DMSO or etoposide. As observed with BT-474 cells, adherent MCF-7 cells incubated with DMSO remained almost 100% viable throughout the culture period. Adherent cells incubated with etoposide decreased in percentage of viable cells with a corresponding increase in percentage of non-adherent viable cells. Again, note that the numbers of viable cells decreased significantly after 40 - 45 hours of incubation (see Figure 9). Also shown in Figure 10 are percentages of apoptotic cells in DMSO- and etoposide-treated cultures. Significantly elevated percentages of apoptotic cells were observed at approximately 22 hours of culture in the presence of etoposide. Percentages of apoptotic cells in these cultures continued to increase thereafter reaching an approximate peak of 58% by 70 hours of incubation.

Figure 11 shows the results of two-parameter flow cytometric analyses of DNA content and 3'-OH-end-labeled fluorescent-positive (apoptotic) MCF-7 cells incubated with DMSO or 85 uM etoposide. Unlike BT-474 cells grown in etoposide in which the total number of apoptotic cells peaked at approximately 20 to 30 hours of culture and decreased significantly thereafter, total numbers of apoptotic MCF-7 cells increased beginning at 16 hours and reached a peak at approximately 40 hours of culture. Similar to BT-474 cells, there was a significant rise in S-phase apoptotic MCF-7 cells during the 16 to 22 hour-culture period but these numbers remained relatively constant throughout the remainder of the culture period. Unlike the rapid increase in numbers of S-phase apoptotic MCF-7 cells described above, significantly elevated numbers of G_0/G_1 and G_2/M apoptotic cells appeared gradually and were significantly lower than those in the S-phase compartment. It was concluded from this series of experiments, that BT-474 cells and MCF-7 cells are both susceptible to the apoptosis-inducing effects of etoposide with some notable differences in the kinetics. In both cases, the highest numbers of apoptotic cells were observed in the S-phase cell cycle compartment although significant numbers of apoptotic cells were also observed in the G_0/G_1 and G_2/M compartments as well.

CONCLUSIONS

Primary human breast cancer tissues obtained from biopsies or mastectomies were characterized in terms of their DNA content by flow cytometric and digital image analyses and for expression of growth factor receptors, e.g. estrogen and progesterone receptors. We were able to analyze one breast cancer biopsy which was accompanied by an axillary lymph node which contained metastatic tumor. The primary (breast) tumor was observed to contain two aneuploid stem lines with DNA indices of 1.4 and 1.9 and S-phase fractions of 19.8% and 7.4%, respectively. Metastatic tumor in the axillary lymph node contained only one aneuploid stem line with an S-phase fraction 9.6% and had a DNA index of 1.7 suggesting the possibility of the emergence of a sub-line in the metastatic tumor. We are currently analyzing frozen and paraffin-embedded tissues from this

patient to clarify the basis for these differences. Future studies in this area will focus on the use of DNA analysis and breast cancer-associated markers (i.e. ER, PR, c-erb-B, adhesion molecules) to characterize primary and metastatic tumors for possible emergence of aneuploid sub-lines.

We were unsuccessful in establishing a xenograft model for growing primary breast cancer tissue explants in immunodeficient (athymic) mice. it appears that, in some cases, tumors did not grow because the implanted specimens were subsequently found to contain either fatty tissue or normal epithelial tissue. In other cases, it is likely that the xenograft failures (later determined to involve ER+ tissues) were due to the lack of a suitable estrogen-enriched environment. Although recipient mice were females, they were not supplemented with estrogen prior to implantation. It has been recently reported that estrogen supplementation enhances tumorigenicity somewhat but a much greater level of tumorigenicity can be obtained when breast cancer cells are co-inoculated with estrogen and basement membrane matrix (Matrigel). In future attempts to grow xenografted primary breast cancer tissue, we will incorporate this approach into our protocol. We were successful in growing two established breast cancer cell lines, BT-474 and DU-4475, as tumor xenografts in nude mice. However, only 10 to 20% of animals injected with these cells developed palpable tumors. It is likely that our success rate in growing xenografted breast cancer cells from established cells lines will also increase when we combine the cell implants with estrogen and basement membrane matrix.

Results of flow cytometric analysis of mutant p53 expression in cell cycle compartments of BT-474, DU-4475 and SK-BR3 cells at various times during a 7-day growth period indicated that, regardless of time in culture and cell cycle compartment, almost all BT-474 cells continually expressed mutant p53 gene product suggesting that the constituitive expression of mutant p53 protein is not modulated by normal growth of BT-474 cells. By contrast, DU-4475 and SK-BR3 cells did exhibit variations in the expression of mutant p53 gene product during their growth. DU-4475 cells exhibited low (16%) percentages of p53 protein expression in all three cell cycle compartments at the initiation of culture. After 1 day of culture, percentages of p53-positive cells rose to 80-90% and then decreased to low (18%) levels after 7 days of culture. Again, all three cell cycle compartments exhibited similar increases and decreases. In DU-4475 cells, there appeared to be no preferential expression in specific phases of the cell cycle. SK-BR3, on the other hand, exhibited a 41% expression of mutant p53 on day 0 which rose to 98.3% by day 1 and remained elevated through day 7. Interestingly, there appeared to be an up-regulation of the expression of this protein in G_0/G_1 and S phases of the cell cycle by day 1, but its expression in G_2/M cells was 96% on day 0 and remained the same throughout the 7-day cuiture period. Since the p53 tumor suppressor gene product has been reported to be involved in the induction of apoptosis as the result of growth factor deprivation possibly by down-regulating bcl-2 expression, we plan to conduct further experiments that are designed to clarify the differences observed in p53 protein expression in the three cell lines described above and to determine how these differences impact on the induction of apoptosis.

A major goal of our research is to establish a model system for studying the involvement of apoptosis in breast cancer cell death. We used a DNA 3'-OH digoxigenin-nucleotide end extension - FITC~anti-digoxigenin labeling technique for detecting the presence of fragmented DNA in intact cell nuclei as a marker for apoptosis. Since DNA fragmentation occurs within a specific time period during apoptosis, this technique does not detect apoptotic cells that are in pre- or post-DNA fragmentation stages. Therefore, a future goal is to combine this technique with other methods of identifying apoptotic cells during all stages of the process. To assess the ability of the 3'-OH end labeling technique to detect apoptotic cells, three breast cancer cell lines were subjected to a

variety of different agents that have been reported to induce apoptosis (hyperthermia, TNF-α, camptothecin, and etoposide). Results of these experiments indicated that the end-labeling method was, indeed, capable of detecting apoptosis in all situations where apoptosis has been detected by other methods.

Adherence is a key growth-requiring characteristic of epithelial-like tumor cell growth in in vitro cultures. Adherent BT-474 cells began decreasing in viable cell numbers by 16 to 23 hours after addition of etoposide to the cultures. Interestingly, there was a corresponding increase in numbers of viable, non-adherent cells in these cultures which peaked at about 40 to 45 hours of incubation and then decreased thereafter. Apparently, the presence of etoposide initially caused a detachment of viable cells between 16 to 23 hours of incubation. A different pattern of cell detachment was observed in the growth of MCF-7 cells incubated with etoposide when compared to growth of non-adherent BT-474 cells. Whereas non-adherent viable BT-474 cells incubated with etoposide exhibited a marked increase in numbers from 16 to 40 hours of culture and decreased thereafter, viable non-adherent MCF-7 cells only exhibited a minimal and gradual increase in number throughout the entire culture period. The basis for this difference between these two cell lines in their detachment patterns when incubated in the presence of etoposide is not clear and is currently under investigation.

Percentages of apoptotic BT-474 and MCF-7 cells increased significantly in etoposide-treated cultures during a 70 hours of incubation. When total numbers were quantitated, however, peak numbers of apoptotic cells were observed at approximately 20 to 30 hours of culture with a significant decline thereafter. This dramatic increase in numbers of apoptotic cells was distributed unequally among G_0/G_1, S and G_2/M cell cycle compartments with the highest number observed in the S-phase. Whereas numbers of apoptotic S-phase cells decreased after 23 to 30 hours of incubation, the numbers of G_0/G_1 and G_2/M apoptotic cells remained at constant levels throughout the remainder of the culture period. These findings are consistent with the S-phase-associated mode of action of topoisomerase inhibitors which primarily affect cells undergoing DNA synthesis and have been shown by Del Bino et al to induce high levels of apoptosis in S-phase HL-60 promyelocytic leukemia cells (26).

We have attempted to established a useful model for continued studies of the involvement of apoptosis in growth regulation of breast cancer cells. The occurrence of exposed 3'-OH DNA ends and their association with apoptosis must be correlated with morphological and biochemical features of apoptosis in order to establish a time-line of its appearance during cell growth. With this model, we will study the influences of growth-promoting and growth-inhibiting factors that modulate the growth of breast cancer cells both in vitro and in vivo.

REFERENCES

1 Clarke PGH, Anat Embryol 181:195, 1990
2 Ellis RE, Curr Opin Genet Devel 2: 635, 1992
3 Ellis RE et al, Ann Rev Cell Biol 7:663 - 698, 1991
4 French-Constant C, Current Biology 2:577, 1992
5 Raff MC, Nature 356:397, 1992
6 Vaux DL, Proc Natl Acad Sci USA 90:786, 1993
7 Wyllie AH, Brit J Cancer 67:205, 1993
8 Whyte, MK et al, J. Immunol. 150:5124, 1993

9 Arend MJ et al, Am. J. Pathol. 136:593, 1990
10 Wyllie AH, Cancer Metast Rev 1:95, 1992
11 Compton MM, Cancer Metast Rev 11:105, 1992
12 Kerr JFR et al, Brit J Cancer 26: 239, 1972
13 Thompson HJ et al, Cancer Epidem Biomarkers and Prevention 1:537, 1992
14 Walker PR et al, Biotechniques 15:1032, 1993
15 Brown DG et al, J Biol Chem 268:3037, 1993
16 Arends MJ et al, Amer J Pathol 136:593, 1990
17 Bursch W et al, Biochem Cell Biol 68:1071, 1990
18 Arends MJ et al, Amer J Pathol 136:593, 1990
19 Gavrieli Y et al, J Cell Biol 119:493, 1992
20 Schmitz, G et al, Anal. Biochem. 192:222, 1991
21 Gorzyca, W et al, Intl. J. Oncol. 1:639, 1992
22 Thiry, M et al, J. Histochem. Cytochem. 40:411, 1992
23 Wijsman, JH et al, J. Histochem. Cytochem. 41:7, 1993
24 Bellomo G et al, Cancer Res. 52:1342, 1992
25 Kyprianou N et al, Cancer Res. 51:162, 1991
26 Del Bino G et al, Leukemia 8:281, 1994
27 Marx J, Science 259:760, 1993
28 Oren M, Cancer Metast 11:141, 1992
29 Hickmann JA, Cancer Metast Rev 11:121, 1992
30 Bertrand R et al, Biochem Pharmacol 42:77, 1991
31 Bertrand R et al, Cancer Res. 51:6280, 1991
32 Lowe SW et al, Nature 362:847, 1993
33 Zhu et al, Brit J Cancer 69:468, 1994
34 Haldar S et al, Cancer Res. 54:2095, 1994
35 Miyashita T et al, Oncogene 9:1799, 1994
36 Price JE et al, Cancer Res. 50:717, 1990
37 van Slooten H-J et al, Brit J. Cancer 72:22, 1995
38 Dressler LG and Bartow SA, Semin. Diagn. Pathol. 6:55, 1989
39 Dressler LG, In Methods to Cell Biology, VoL 33, pgs 157-171, Darzynkiewiczk Z and Crissman H, eds., Academic Press, New York, 1990
40 Lasfargues E and Coutinho WG, J. Natl. Cancer Inst. 61: 967, 1978
41 Soule HD et al, J. Natl. Cancer Inst. 51: 1409, 1973
42 Cailleau R et al, J. Natl. Cancer Inst. 53:661, 1974
43 Langlois AJ et al, Cancer Res. 39: 2604, 1979
44 Lowe SW et al, Nature 362: 847, 1993
45 Bartek J et al, Oncogene 5:893, 1990

APPENDIX

TABLES 1 - 8

FIGURES 1 - 11

TABLE 1. PRIMARY HUMAN BREAST TUMORS

TISSUE #	DIAGNOSIS	ER*	PR*
TI0001	MODERATELY DIFFERENTIATED DUCTAL ADENOCARCINOMA (RESIDUAL)	NEG	NEG
TI0004	INFILTRATING DUCTAL CARCINOMA	60%	40%
TI0007	INFILTRATING DUCTAL CARCINOMA, GRADE II	70%	NEG
TI0008	LYMPH NODE OF TI0007	ND	ND
TI0009	MULTI-FOCAL INTRADUCTAL CARCINOMA (RESIDUAL)	NEG	NEG
TI0010	MODERATELY DIFFERENTIATED INFILTRATING DUCTAL CARCINOMA	80%	NEG
TI0012	DUCTAL, INTRADUCTAL, INFILTRATING CARCINOMA	50%	NEG
TI0014	FOCAL, INTRADUCTAL MEDULLARY CARCINOMA	NEG	NEG
TI0018	INFILTRATING DUCTAL CARCINOMA, GRADE III (BIOPSY)	± 10%	NEG
TI0023	INFILTRATING DUCTAL CARCINOMA, GRADE III (BIOPSY)	80%	90%
TI0024	MODIFIED RADICAL MASTECTOMY OF TI0023	80%	90%
TI0025	NORMAL BREAST TISSUE OF TI0023	ND	ND
TI0026	MODERATELY DIFFERENTIATED MULTI-FOCAL INFILTRATING DUCTAL CARCINOMA	40%	NEG
TI0027	INFILTRATING DUCTAL CARCINOMA	ND	ND
TI0028	MODERATELY DIFFERENTIATED INFILTRATING DUCTAL CARCINOMA	NEG	70%
TI0030	INFILTRATING DUCTAL CARCINOMA, GRADE III	NEG	NEG
TI0031	INFILTRATING DUCTAL CARCINOMA, GRADE III	NEG	30%
TI0033	INFILTRATING LOBULAR CARCINOMA (RESIDUAL)	80%	60%
TI0036	INFILTRATING DUCTAL CARCINOMA, GRADE II	NEG	NEG

* ER = estrogen receptor; PR = progesterone receptor; NEG = < 10%; ND = not determined

TABLE 2. FLOW CYTOMETRIC ANALYSIS OF PRIMARY HUMAN BREAST TUMORS

	NORMAL/DIPLOID CELLS				STEM 1 ANEUPLOID CELLS					STEM 2 ANEUPLOID CELLS				
TISSUE #	%DIPL	G0/G1	S	G2/M	%ANEU	G0/G1	S	G2/M	DI	%ANEU	G0/G1	S	G2/M	DI
NORMAL	100	98	1	1	-	-	-	-	-	-	-	-	-	-
TI0001	100	98	2	0	SAMPLE INADEQUATE; NO ANEUPLOID CELLS DETECTED									
TI0004	100	96	3	1	SAMPLE INADEQUATE; NO ANEUPLOID CELLS DETECTED									
TI0007	20	97	1	2	34	77	20	3	1.4	46	90	7	3	1.9
TI0008	75	97	2	1	25	87	10	3	1.7	-	-	-	-	-
TI0009	100	97	1	2	SAMPLE INADEQUATE; NO ANEUPLOID CELLS DETECTED									
TI0012	83	97	2	1	17	85	14	1	1.8	-	-	-	-	-
TI0014	74	98	1	1	26	82	11	7	1.5	-	-	-	-	-
TI0018	48	..	3	0	52	86	9	5	1.9	-	-	-	-	-
TI0023	16	97	1	2	84	78	11	11	1.8	-	-	-	-	-
TI0025	100	96	2	2	SAMPLE INADEQUATE; NO ANEUPLOID CELLS DETECTED									
TI0026	100	96	3	1	SAMPLE INADEQUATE; NO ANEUPLOID CELLS DETECTED									
TI0027	61	98	2	0	39	38	46	16	1.6	-	-	-	-	-
TI0028	42	97	2	1	58	92	4	4	1.8	-	-	-	-	-
TI0030	60	99	1	0	40	85	11	4	1.8	-	-	-	-	-
TI0031	43	96	3	1	57	83	8	9	1.5	-	-	-	-	-
TI0033	100	98	1	1	SAMPLE INADEQUATE; NO ANEUPLOID CELLS DETECTED									
TI0036	100	96	9	1	SAMPLE INADEQUATE; NO ANEUPLOID CELLS DETECTED									

TABLE 3. IMAGE ANALYSIS OF NORMAL HUMAN BREAST EPITHELIAL CELLS, HUMAN PERIPHERAL BLOOD MONONUCLEAR CELLS AND NORMAL RAT HEPATOCYTES

NORMAL TISSUE	NO. TESTED	PREPARATION	MEAN IOD + SD
NORMAL BREAST EPITHELIAL CELLS	16	FRESH	163.5 ± 3.4
NORMAL PERIPHERAL BLOOD MONONUCLEAR CELLS	5	FRESH	158.3 ± 1.6
NORMAL RAT HEPATOCYTES	13	FRESH	134.1 ± 1.0
NORMAL BREAST EPITHELIAL CELLS	5	FRESH / TOUCH	162.4 ± 2.5
NORMAL BREAST EPITHELIAL CELLS	5	FRESH / MECHANICAL	164.6 ± 4.3
NORMAL BREAST EPITHELIAL CELLS	5	FROZEN / TOUCH	159.7 ± 4.7
NORMAL BREAST EPITHELIAL CELLS	5	FROZEN / MECHANICAL	163.9 ± 2.0

* IOD = integrated optical density

STATISTICS:

Normal Breast Epithelial Cells vs. Peripheral Blood Mononuclear Cells:	Significant Difference at P = 0.0041
Normal Breast Epithelial Cells vs. Rat Hepatocytes:	Significant Difference at P < 0.0001
Normal Peripheral Blood Mononuclear Cells vs. Rat Hepatocytes:	Significant Difference at P < 0.0001
Fresh vs Frozen and Touch Imprint vs. Mechanical:	No Significant Difference at P = 0.05

TABLE 4. IMAGE ANALYSIS OF EVALUABLE PRIMARY HUMAN BREAST TUMORS

	REF-IOD		MEAN IOD OF ANEUPLOID CELLS			% OF TOTAL ANEUPLOID CELLS			DNA INDEX		
TISSUE	EXT	INT	G0 / G1	S	G2 / M	G0 / G1	S	G2 / M	EXT	INT	5c Exceed
TI0001	164	156	514	707	1027	82	11	7	3.1	3.3	46.4
TI0004	164	-	165	241	337	94	1	5	1.0	-	0.0
TI0007 (Stem 1)	164	158	209	370	422	79	18	3	1.3	1.3	1.3
TI0007 (Stem 2)	164	158	303	438	596	89	8	3	1.9	1.9	2.7
TI0008	164	157	288	403	568	87	9	4	1.8	1.8	2.4
TI0012	164	165	290	377	563	85	12	3	1.8	1.8	2.1
TI0014	164	164	226	315	453	78	12	10	1.4	1.4	16.9
TI0018	164	165	296	437	590	83	10	7	1.8	1.8	13.6
TI0023	164	162	285	397	554	75	13	12	1.7	1.8	15.1
TI0024	164	-	161	238	331	96	2	2	1.0	-	0.0
TI0026	164	-	167	237	331	[illegible]	4	5	1.0	-	0.0
TI0028	164	167	302	383	604	85	9	6	1.8	1.8	7.3
TI0030	164	162	298	380	588	81	14	5	1.8	1.8	6.4
TI0031	164	168	253	360	498	73	17	10	1.5	1.5	11.8

* REF-IOD EXT = mean integrated optical density of human breast epithelial cells from normal breast tissue biopsy;
REF-IOD INT = mean integrated optical density of normal breast epithelial cells within tumor sample

TABLE 5. FLOW CYTOMETRIC AND IMAGE ANALYSES OF HUMAN BREAST CANCER CELL LINES

CELL LINE	CULTURE CONDITIONS	EXT REF IOD	MEAN IOD OF ANEUPLOID CELLS G0 / G1	S	G2 / M	% OF ANEUPLOID CELLS G0 / G1	S	G2 / M	DI	5c Exceed
SK-BR3	10 mg/L L-alanine 10% FBS	164	360	515	722	68 (69)	17 (18)	15 (13)	2.2 (2.3)	31.2
MDA-MB-231	10% FBS	164	405	562	810	40 (NT)	34 (NT)	26 (NT)	2.5 (NT)	68.0
BT-474	10 mg/L insulin 300 mg/L L-glutamine 10% FBS	164	441	650	879	71 (80)	18 (24)	11 (6)	2.7 (2.6)	94.9
DU4475	20% FBS	164	323	470	638	70 (73)	17 (16)	13 (11)	2.0 (2.1)	38.1
TI0016 (DU-4475)	Nude Mouse Tumor	164	327	430	657	64 (61)	22 (25)	14 (14)	2.0 (2.1)	19.4

* ( ) = values in parentheses represent determinations by flow cytometric analyses
EXT REF IOD = mean integrated optical density of human breast epithelial cells from normal breast tissue biopsy

TABLE 6. IMAGE ANALYSES OF BT-474 CELLS GROWN IN THE PRESENCE OR ABSENCE OF INSULIN

DAYS OF CULTURE	VIABLE CELLS X 10^5 NON-ADHERENT + INS	NON-ADHERENT - INS	ADHERENT + INS	ADHERENT - INS	MEAN IOD OF ANEUPLOID CELLS G0 / G1	S	G2 / M	% OF ANEUPLOID CELLS G0 / G1	S	G2 / M	DI
6 HOURS	0.05	0.08	9.3	10.1	369	550	786	67	24	9	2.3
1	0.07	0.10	12.3	10.5	378	515	730	69	21	10	2.3
2	0.02	0.19	22.3	11.7	387	561	764	73	16	11	2.4
3	0.06	0.66	34.3	16.3	401	556	803	59	21	20	2.5
4	0.02	1.3	42.7	25.8	415	588	823	66	16	18	2.5
7	0.23	2.5	70.0	39.2	420	528	836	65	16	19	2.6
9	0.20	3.1	143.3	58.4	404	594	798	72	14	14	2.5
11	0.47	5.7	120.0	44.6	428	629	854	76	12	12	2.6

* DI = DNA indices which were calculated with a reference mean IOD value for normal breast epithelial cells of 163.5
+ INS = 10 mg/L bovine insulin added to culture medium; - INS = no insulin added to culture medium

TABLE 7. FLOW CYTOMETRIC ANALYSIS OF THE EXPRESSION OF MUTANT p53 GENE PRODUCT IN BT-474, SK-BR3, AND DU-4475 CELLS

CELLS	DAYS OF CULTURE	% OF TOTAL CELLS p53+	% OF TOTAL CELLS IN EACH CELL CYCLE COMPARTMENT			% OF p53+ CELLS IN EACH CELL CYCLE COMPARTMENT		
			G0 / G1	S	G2 / M	G0 / G1	S	G2 / M
BT-474	0	95	70	22	8	94	99	99
BT-474	1	92	67	24	9	92	93	92
BT-474	3	96	72	16	12	95	93	98
BT-474	7	97	80	10	10	97	99	99
DU-4475	0	16	82	13	5	13	38	34
DU-4475	1	86	68	10	22	82	94	95
DU-4475	3	68	81	10	9	67	76	88
DU-4475	7	19	82	11	7	17	48	23
SK-BR3	0	41	87	6	7	34	72	96
SK-BR3	1	98	69	21	10	98	99	99
SK-BR3	3	87	75	16	9	82	91	98
SK-BR3	7	95	86	8	6	95	97	98

* Mutant p53 expression determined by labeling cells with monoclonal FITC-anti-p53 clone 240 (Dako) DNA analysis by propidium iodide staining

TABLE 8. INDUCTION OF APOPTOSIS BY HEAT, CAMPTOTHECIN, ETOPOSIDE AND TNF-α IN BT-474 CELLS, MCF-7 CELLS AND DU-4475 CELLS

TREATMENT	INCUBATION TIME	% APOPTOTIC CELLS BT-474 CELLS	DU-4475 CELLS	MCF-7 CELLS
DNase (1 ug)*	10 MINUTES	98	94	94
NONE	18 HOURS	2	-	-
43°C for 15 MINUTES	18 HOURS	53	-	-
43°C for 30 MINUTES	18 HOURS	52	-	-
43°C for 45 MINUTES	18 HOURS	49	-	-
43°C for 60 MINUTES	18 HOURS	65	-	-
PBS	6 HOURS	-	9	-
DMSO	6 HOURS	-	11	-
1 ng/ml TNF-α	6 HOURS	-	10	-
10 ng/ml TNF-α	6 HOURS	-	12	-
100 ng/ml TNF-α	6 HOURS	-	31	-
PBS	6 HOURS	-	7	-
DMSO	6 HOURS	-	11	-
0.1 uM CAMPTOTHECIN	6 HOURS	-	33	-
0.15 uM CAMPTOTHECIN	6 HOURS	-	26	-
0.2 uM CAMPTOTHECIN	6 HOURS	-	28	-
PBS	18 HOURS	5	9	-
DMSO	18 HOURS	13	13	-
0.1 uM CAMPTOTHECIN	18 HOURS	16	35	-
0.15 uM CAMPTOTHECIN	18 HOURS	30	31	-
0.2 uM CAMPTOTHECIN	18 HOURS	27	24	-
PBS	6 HOURS	7	-	5
DMSO	6 HOURS	5	-	7
85 uM ETOPOSIDE	6 HOURS	7	-	3
PBS	18 HOURS	6	-	6
DMSO	18 HOURS	6	-	8
85 uM ETOPOSIDE	18 HOURS	30	-	15
PBS	24 HOURS	4	-	6
DMSO	24 HOURS	7	-	7
85 uM ETOPOSIDE	24 HOURS	41	-	21
PBS	30 HOURS	7	-	7
DMSO	30 HOURS	8	-	9
85 uM ETOPOSIDE	30 HOURS	48	-	31
PBS	45 HOURS	5	-	7
DMSO	45 HOURS	10	-	13
85 uM ETOPOSIDE	45 HOURS	62	-	45

* DNase = positive control samples treated with 1 ug/ml DNase for 10 minutes

FIGURE 1
ESTROGEN RECEPTOR^{+}
INTRADUCTAL CARCINOMA

FIGURE 2

BT-474 + DMSO

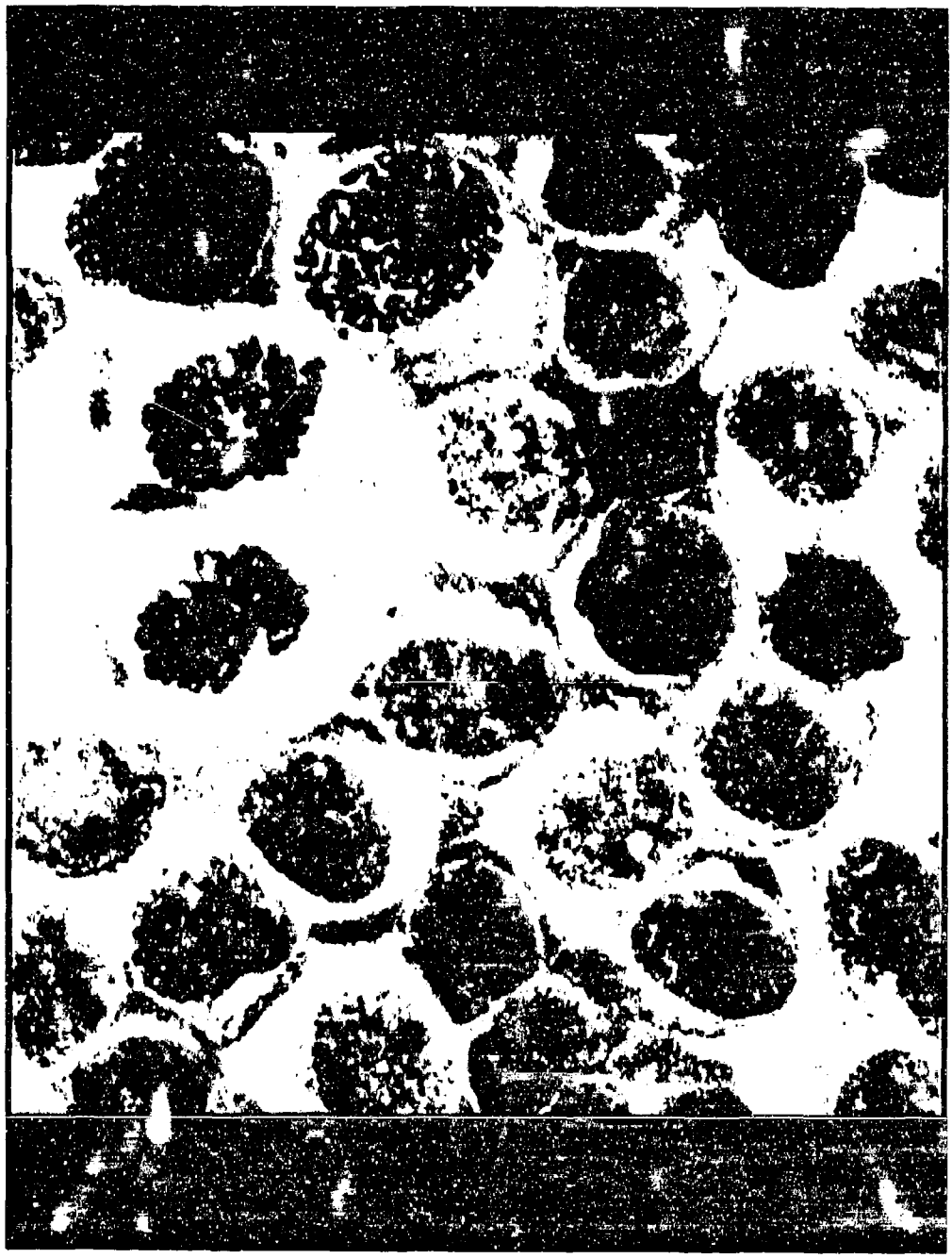

FIGURE 3
BT-474 + ETOPOSIDE
EARLY APOPTOSIS

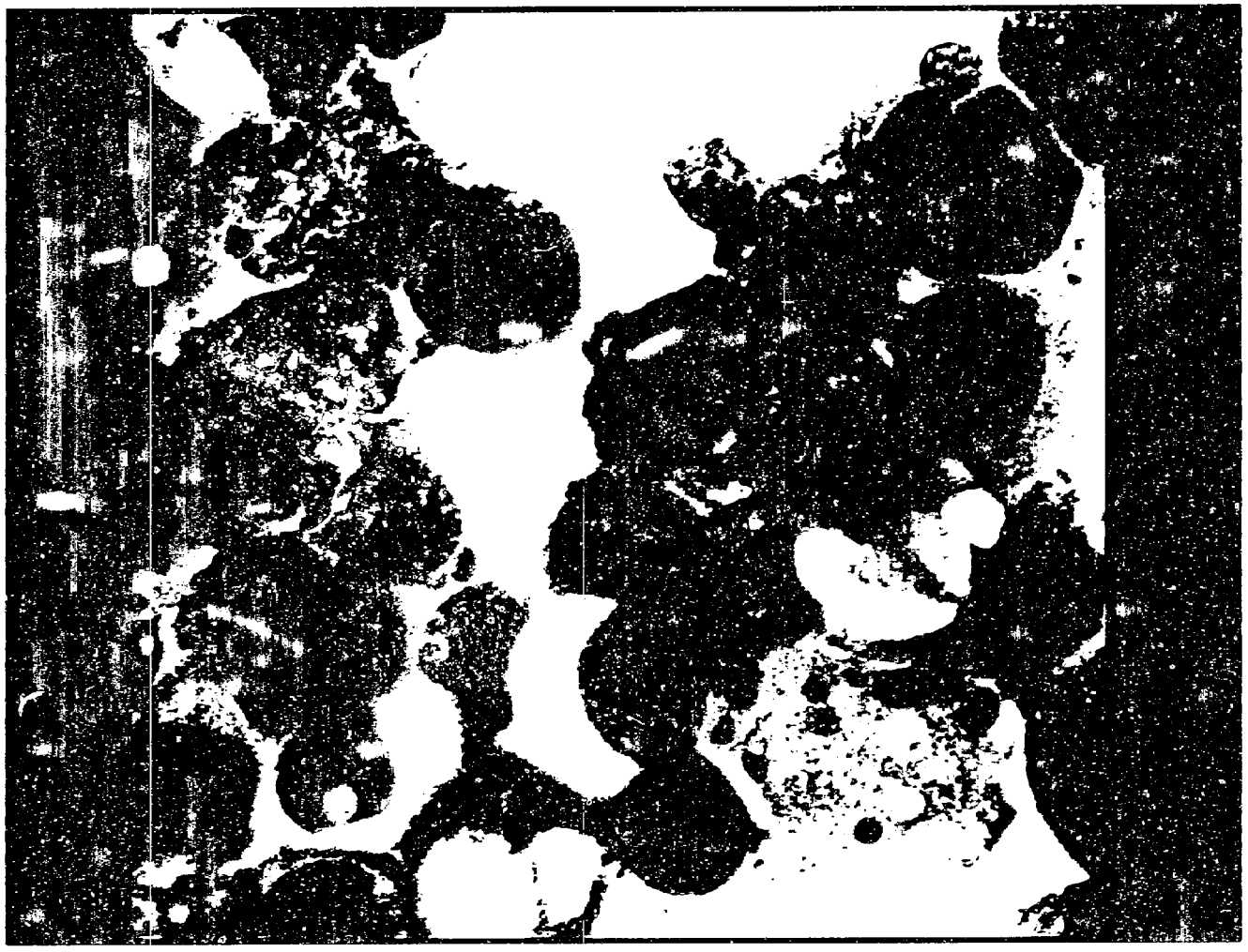

FIGURE 4
BT-474 + ETOPOSIDE
ADVANCED APOPTOSIS

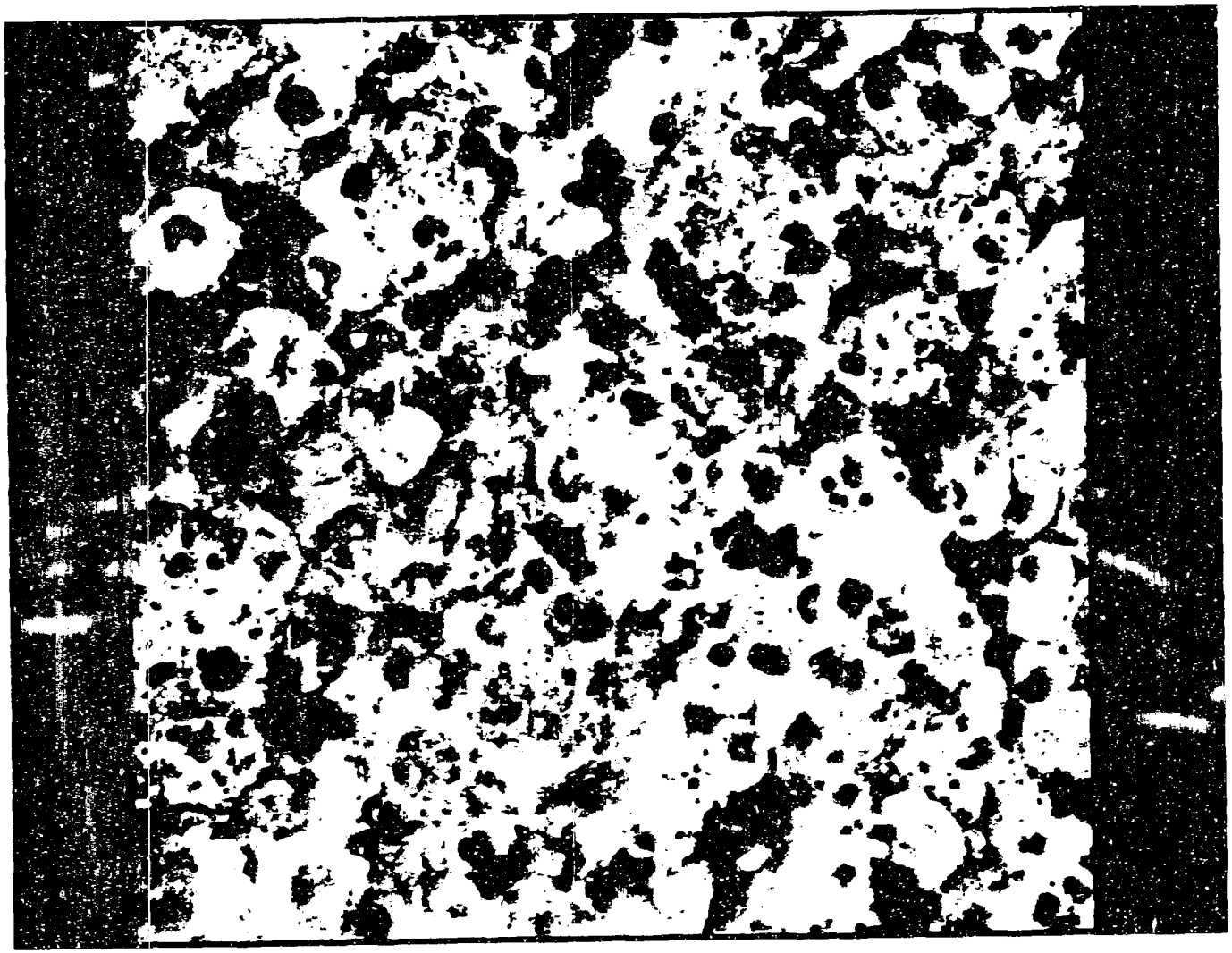

FIGURE 5. BT-474 CELLS INCUBATED WITH ETOPOSIDE: NUMBER OF VIABLE CELLS

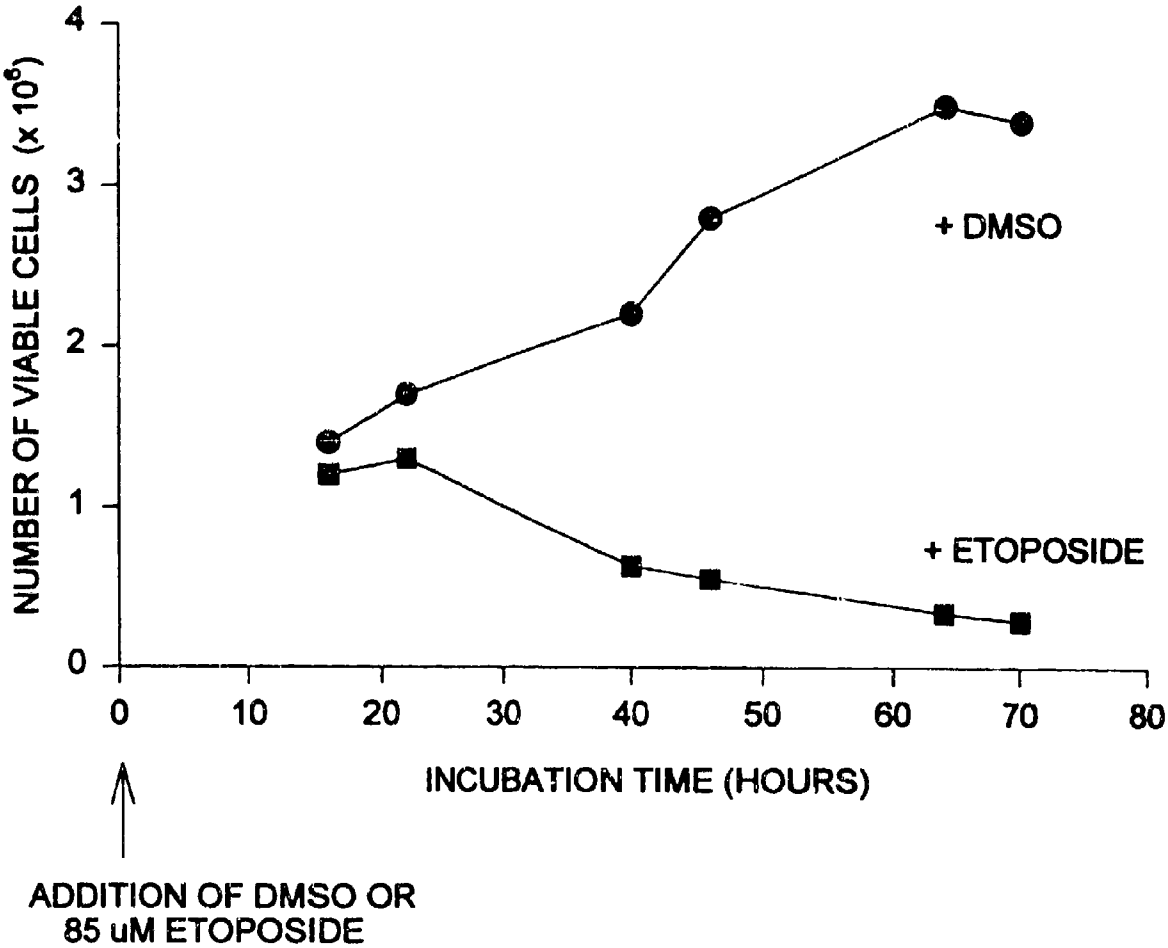

FIGURE 6. BT-474 CELLS INCUBATED WITH ETOPOSIDE: NUMBER OF VIABLE ADHERENT AND NON-ADHERENT CELLS

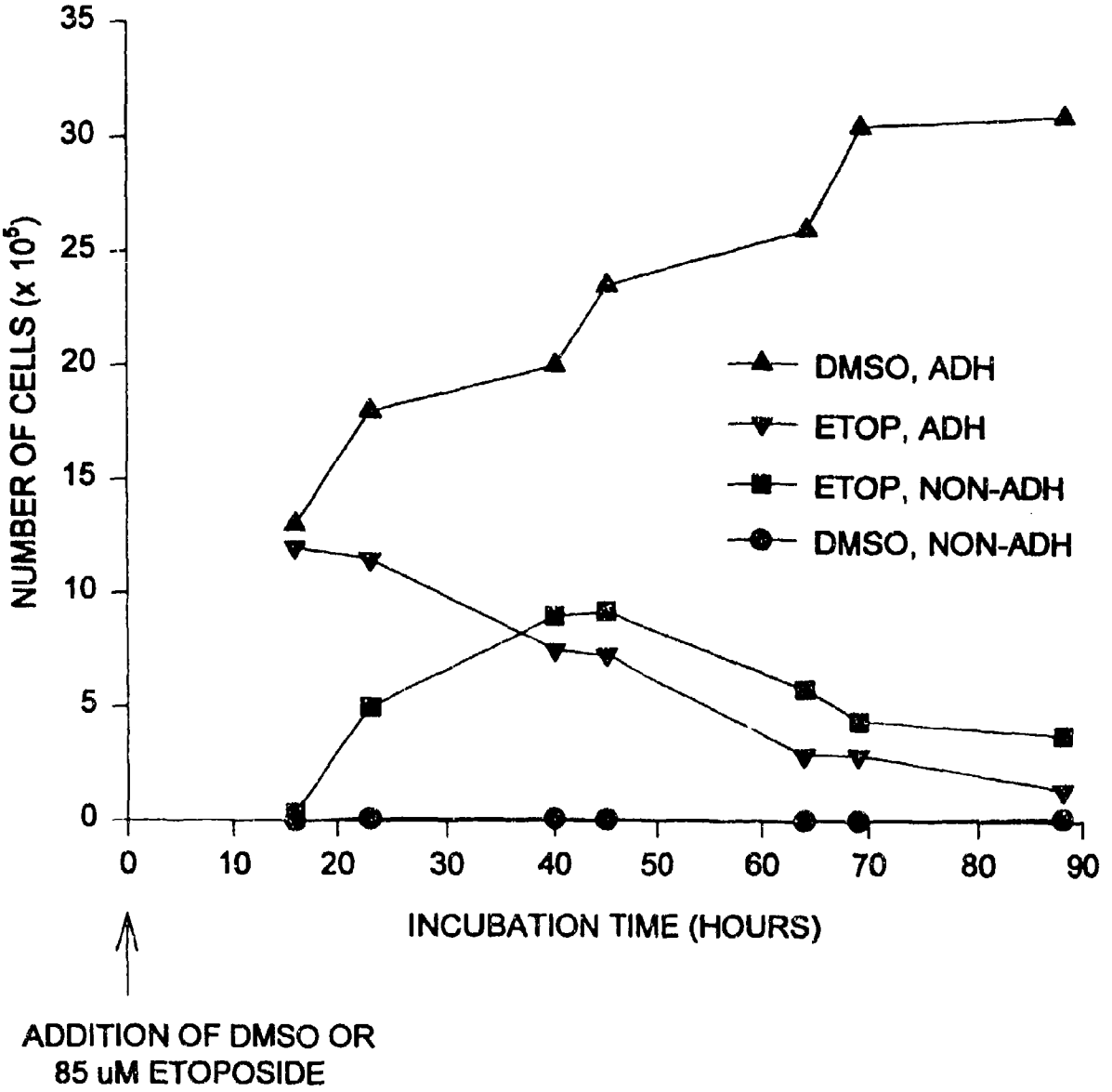

FIGURE 7. BT-474 CELLS INCUBATED WITH ETOPOSIDE: PERCENT OF VIABLE ADHERENT AND NON-ADHERENT CELLS

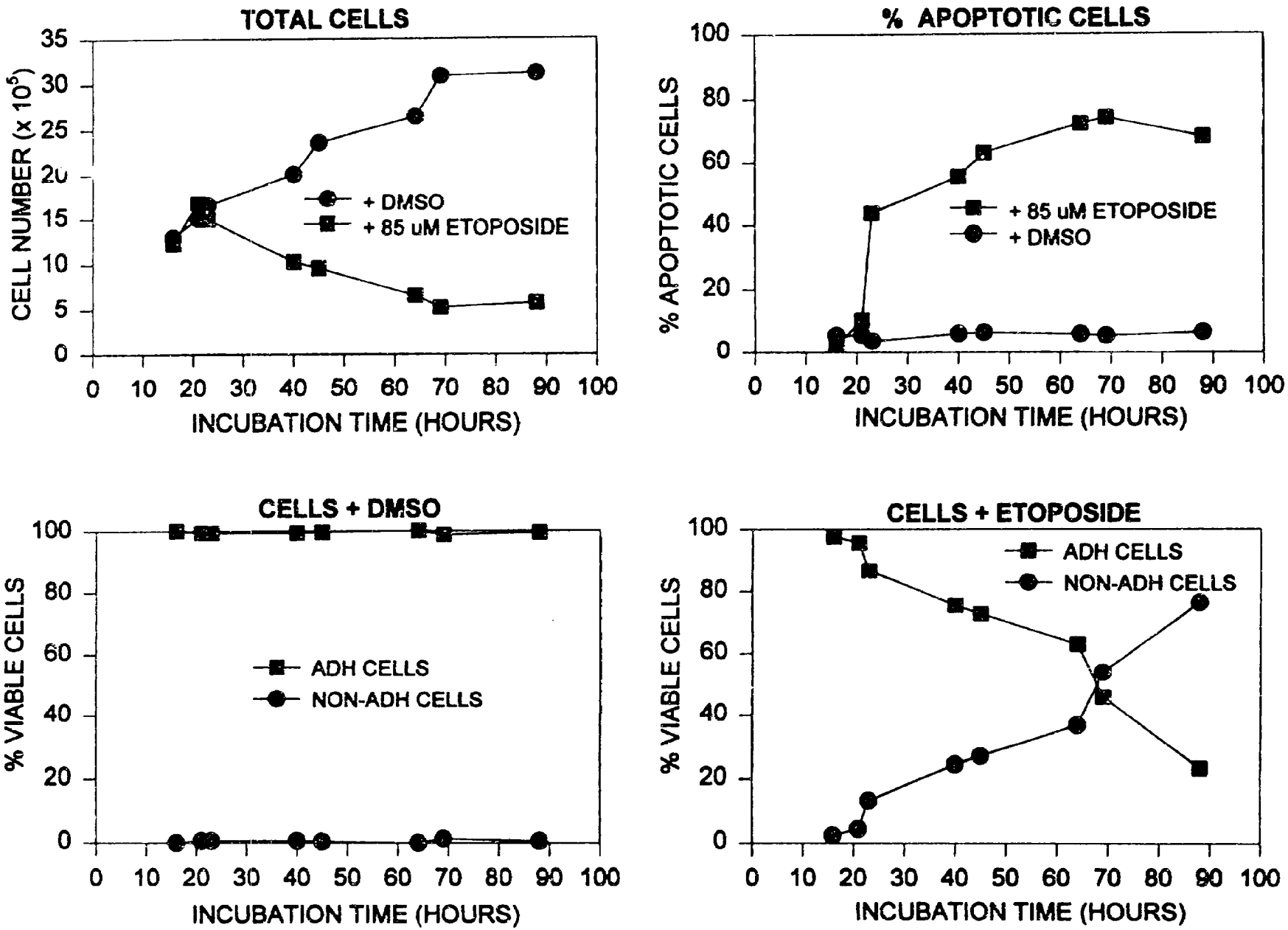

FIGURE 8. BT-474 CELLS INCUBATED WITH ETOPOSIDE: NUMBER OF APOPTOTIC CELLS IN CELL CYCLE COMPARTMENTS

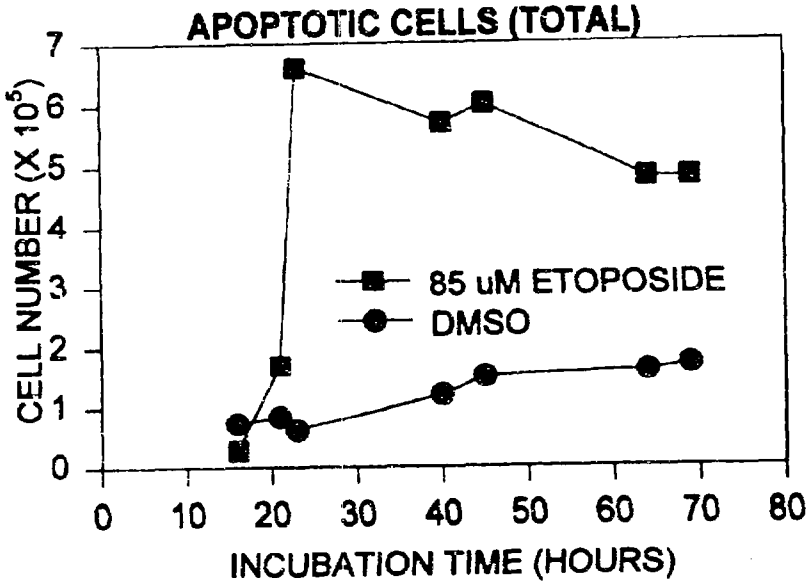

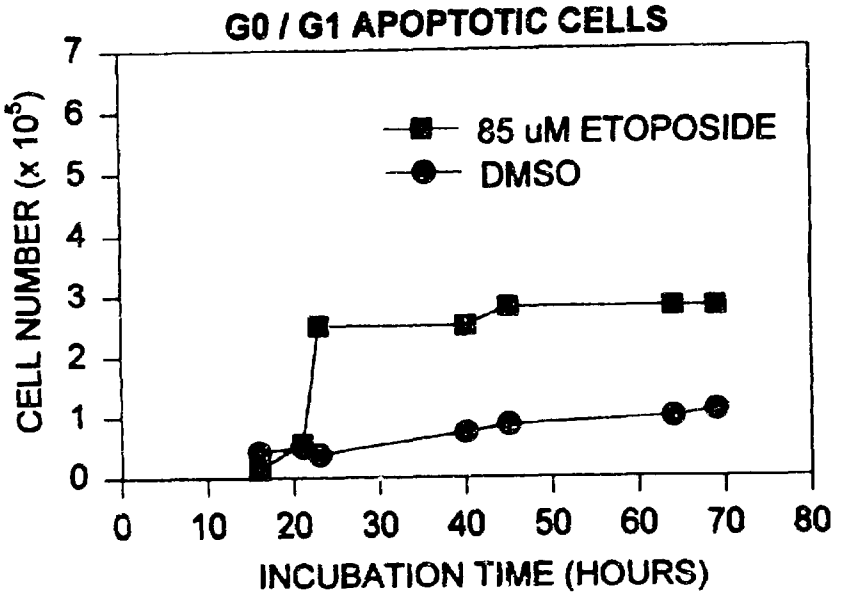

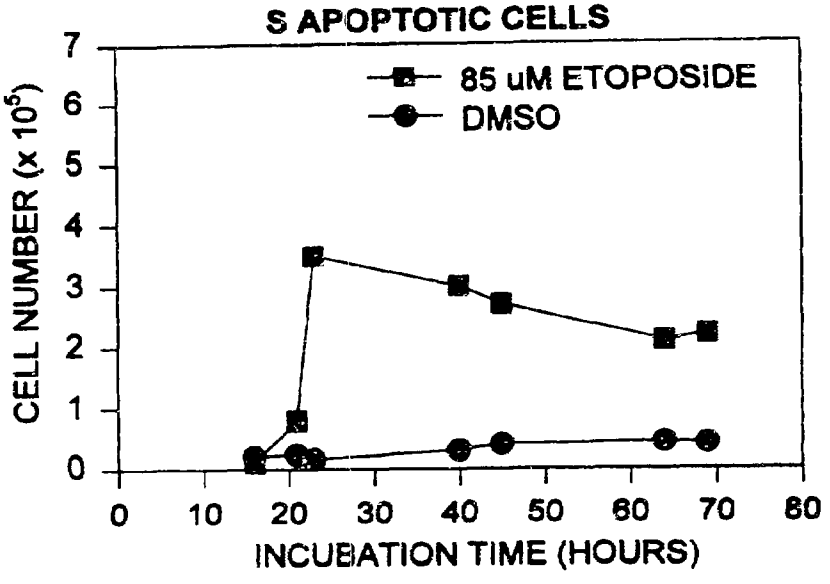

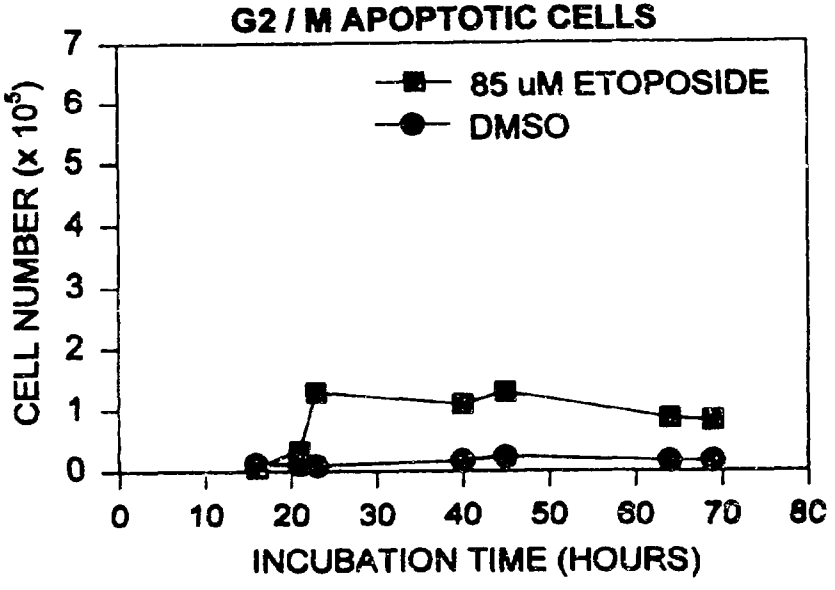

FIGURE 9. MCF-7 CELLS INCUBATED WITH ETOPOSIDE: NUMBER OF VIABLE ADHERENT AND NON-ADHERENT CELLS

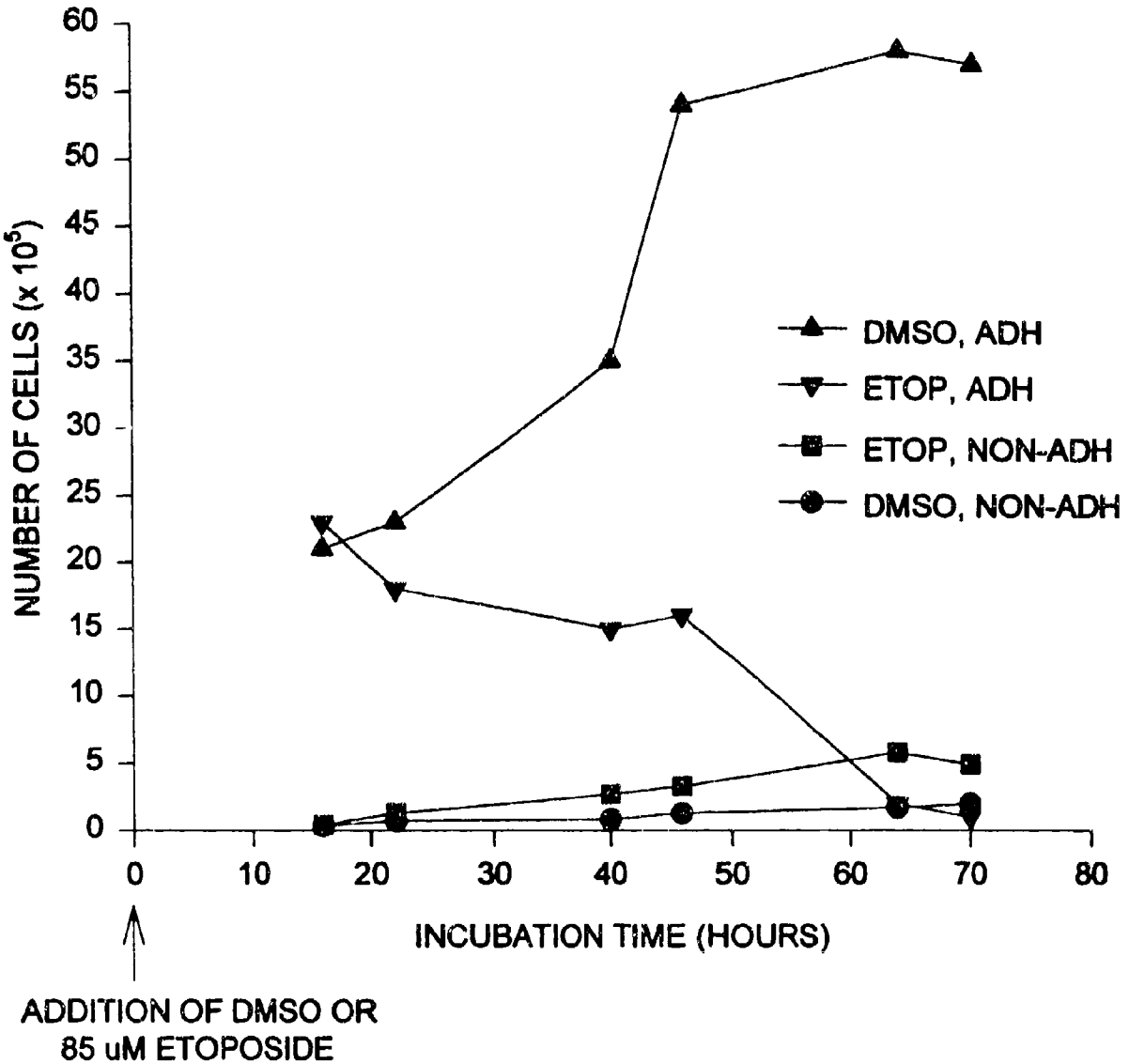

FIGURE 10. MCF-7 CELLS INCUBATED WITH ETOPOSIDE: PERCENT OF VIABLE ADHERENT AND NON-ADHERENT CELLS

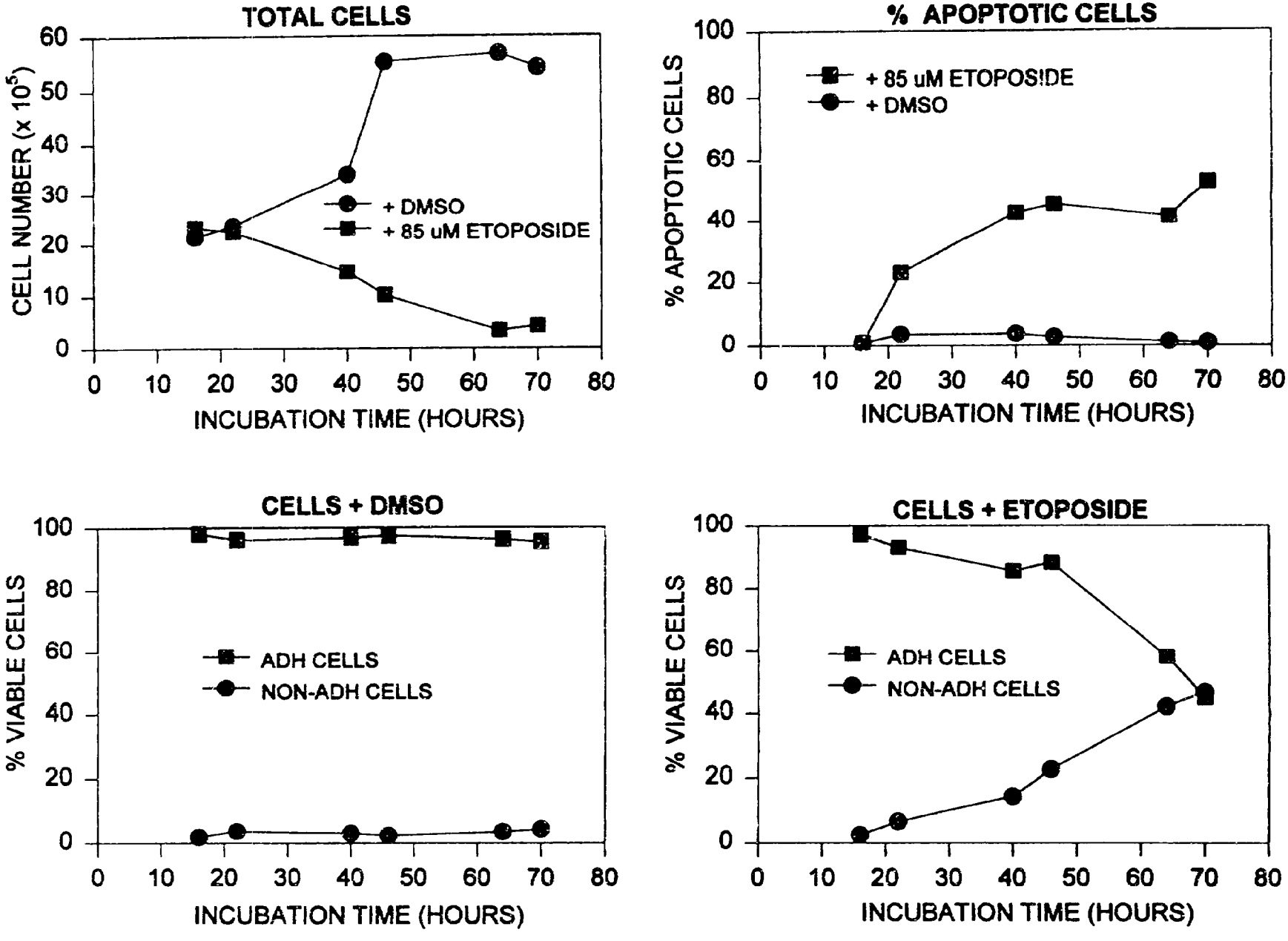

FIGURE 11. MCF-7 CELLS INCUBATED WITH ETOPOSIDE: NUMBER OF APOPTOTIC CELLS IN CELL CYCLE COMPARTMENTS